Prediction of Combustion in Spark Ignition Engine by Simulation Model

Seiko Kono, Hiroaki Motooka and Akihito Nagao
Mazda Motor Corp., Hiroshima

ABSTRACT

By developing the phenomenological combustion model of a spark ignition engine and measuring the in-cylinder flow by means of Hot Wire anemometer, the influences of gas flow or residual gas on burning velocity and the flame thickness have been studied in calculation. As for measuring in-cylinder flow, flow at the piston crown was also measured using the Link Method. Predictions of the in-cylinder flow model, which is made by coupling the K-ε model and the wall shear, are in agreement with the flow at the piston crown. The flame thickness has been obtained using the characteristics of the turbulent entrainment model, and these calculations are fairly reasonable. It's verified that these models represent the combustion phenomena well. Furthermore, influences of a few but representative parameters on thermal efficiency have been investigated. These results offer us an indicator for engine development.

INTRODUCTION

Recently, because of the demand to reduce fuel consumption, the in-cylinder flow characteristics of swirl and squish and the geometrical flame propagation characteristics concerned with for example, spark plug location and combustion chamber shape have been used and combined in the best possible way to improve engine combustion and to develop a spark ignition engine.

In the processes of these studies, the need to research the phenomena of in-cylinder flow and combustion structure in more detail has arisen.

In terms of modeling, a sophisticated multi-dimensional model has been made that incorporates the complex shape of the combustion chamber (1), (2).

To develop a multi-dimensional model, however, requires enormous time and effort. In any case, the main purpose of this study was first to grasp combustion phenomena, and then to develop a phenomenological model.

Because in-cylinder flow is a principal factor of combustion, in-cylinder flow has been measured by Hot Wire anemometer which is simple to use and gives us a highly accurate signal of turbulence, though it is a classical method. In-cylinder flow data which were obtained by Hot Wire anemometer have been used not only to understand the problem but also to make a model.

As for combustion structure, turbulent flame thickness has been calculated by utilizing the characteristics of the turbulent entrainment model. The influences of turbulence and residual gas on combustion structure have also been investigated.

The influences of in-cylinder flow and residual gas on combustion and thermal efficiency, and so on, have been grasped. The results of our work are reported in this paper.

ENGINE SIMULATION MODEL

This simulation model is based on the turbulent entrainment model, and is combined with induction & exhaust, in-cylinder flow, combustion, flame propagation and emissions subprograms as shown in Fig. 1.

Each model is discussed below.

Induction & Exhaust Model

The quasi-steady flow model which is well-known is used (3). The following assumptions are made:

1) Constant pressure and temperature in induction and exhaust manifolds
2) Infinite plenum manifolds
3) Disregard acceleration effects of the gas

The flow rate through the valves is given by eqs. (1) and (2)

$$\frac{dMi}{dt} = Av,i\ Pu\left\{\frac{2}{RTu}\frac{\gamma}{\gamma-1}\left(\frac{P}{Pu}\right)^{\frac{2}{\gamma}}\left[1-\left(\frac{P}{Pu}\right)^{\frac{\gamma}{\gamma-1}}\right]\right\}^{1/2} \quad (1)$$

under conditions of choked flow, that is

$$\frac{P}{Pu} \leqslant \left(\frac{2}{\gamma+1}\right)^{\frac{\gamma}{\gamma-1}}$$

eq. (1) is changed to eq. (2).

$$\frac{dMi}{dt} = Av,i\ Pu\left\{\frac{2}{RTu}\frac{\gamma}{\gamma+1}\left(\frac{2}{\gamma+1}\right)^{\left(\frac{\gamma}{\gamma-1}\right)}\right\}^{1/2} \quad (2)$$

where subscript u refers to upstream conditions, subscript i indicates induction or exhaust. Av,i is the instantaneous effective open valve area, and is represented by a multiple of the open valve area and the flow coefficient. The flow coefficient which is written as a linear function of L/D (=(valve lift)/(valve diameter)) was given to agree with a measured volumetrical efficeincy under such a condition as 1500 rpm and wide open throttle (3), (4).

Conservation of energy for an open system is written as follows:

$$\dot{E} = \dot{Q} - \dot{W} + \dot{H}in\dot{M}in + \dot{H}ex\dot{M}ex \qquad (3)$$

Assuming no kinetic or potential energy contributions, the internal energy equation is represented by eq. (4).

$$\dot{E} = \dot{H}c\dot{M}c + \dot{H}c\dot{M}c - \dot{P}c\dot{V}c - \dot{P}c\dot{V}c \qquad (4)$$

where subscript c refers to cylinder.

Using eqs. (1)-(4) and the perfect gas law, we can calculate the pressure, temperature and mass in the cylinder.

The residual gas fraction is calculated, under the assumption that the whole residual gas, which backflows into the intake manifold during overlap, flows into the cylinder again.

In-cylinder Flow Model

In-cylinder flow is constructed by the mean flow field characterized by swirl and the turbulence field characterized by turbulence. The three dimensional Navie-Stokes equation has to be solved if we need perfect predictions of 3-D in-cylinder flow. The simplified mean flow model and the K-ε turbulence model with the wall shear which have been proposed by Borgnakke, Davis et al. (5), (6), however, give us good predictions of swirl and turbulence.

In these models, the following assumptions are made:

1) Quasi-steady flow during the induction stroke
2) Axially symmetric flow and non-solid body swirl
3) Compressible, unsteady and uniform turbulence field

Angular momentum equation for an open system is described simply as follows.

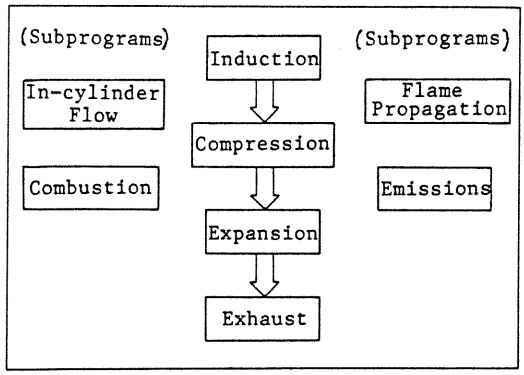

Fig.1 Structure of Engine Simulation Model

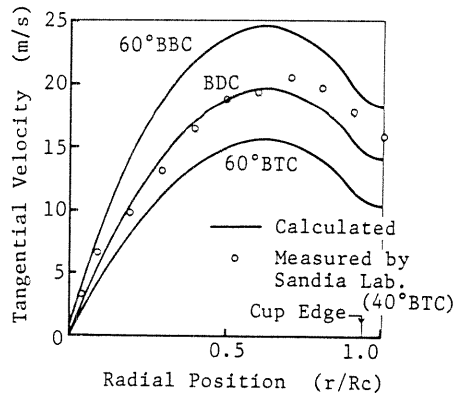

Fig.2 Comparison of Swirl Profile

$$\frac{d}{dt}(M\cdot\Omega) = Ts + \dot{M}in\Omega in - \dot{M}ex\Omega ex \qquad (5)$$

where Ts is the shear stress tensor. The decrease of angular momentum by wall and air friction is considered (5).

The swirl profile is important to calculate the decrease of angular momentum and turbulence. In this study, the swirl profile is given as eq. (6); (5).

$$U_\theta = \begin{cases} ar^2 + br & r < Rb \\ c + dr^{-1} & r > Rb \end{cases} \qquad (6)$$

The following assumptions are made to decide the four constants in eq. (6), referring to the measurements of Sandia (5).

$$U\theta(\tfrac{2}{3}Rb) = Max[U\theta(r)] \qquad (7)$$

$$U\theta(Rc) = U\theta(\tfrac{1}{4}Rb) \qquad (8)$$

where Rb and Rc are radius of cavity and cylinder. Fig. 2 shows the swirl profile of both the calculations and the measurements of Sandia.

On the above mean flow field, the K-ε turbulence model which is given by eqs. (9) and (10) has been applied (21).

$$\rho(dK/dt) = Pk - Dk + Jk \qquad (9)$$

$$\rho(d\varepsilon/dt) = P\varepsilon - D\varepsilon + J\varepsilon \qquad (10)$$

where P is a production, D is a destruction and J is a diffusion term of structure.

A production term is constructed by a compression, a shear stress and an induction term as eq. (11); (5).

$$Pk = \frac{2}{3}K\frac{d\rho}{dt} + \rho\nu t\left(\frac{\partial U\theta}{\partial r} - \frac{U\theta}{r}\right)^2 + \frac{\dot{M}in}{V}(Kin - K) \qquad (11)$$

where νt is a turbulent kinematic viscosity which is defined as eq. (12).

$$\nu t = C\nu K^2/\varepsilon \quad , \quad C\nu = 0.09 \qquad (12)$$

Using this coefficient $C\nu$, the integral length scale is defined by the following equation.

$$L = C\nu^{3/4} K^{3/2} /\varepsilon \qquad (13)$$

After ignition, the turbulence intensity and the integral length scale are given as the following which were developed by Tabaczynski et al. (7).

$$u' = u'o\ (\rho u/\rho u_0)^{1/3} \tag{14}$$

$$L = L\ o\ (\rho u_0/\rho u)^{1/3} \tag{15}$$

where u' is the turbulence intensity, which is equal to $\sqrt{K}$, and where subscript o refers to the end of ignition delay.

Combustion Model

Thermodynamics. Considering the two zones of burned & unburned gas and the inflow & outflow gas of each zone, the thermodynamics equations of each zone for an open system can be constructed (8).

. Energy conservation

$$\dot{E}i = \dot{Q}i - \dot{W}i - Hin,i \cdot Min,i + Hout,i \cdot Mout,i \tag{16}$$

. Internal energy equation

$$Ei = MiHi - PV \tag{17}$$

. Work & enthalpy

$$\dot{W}i = P\dot{V}i,\ \dot{H}i = Cp,i(T)\dot{T}i \tag{18}$$

. Mass conservation

$$\dot{M}b + \dot{M}u = 0 \tag{19}$$

. Entrainment

$$Me = Min,b = - Mout,u \tag{20}$$

where a subscript i refers to b (burned) or u (unburned). The heat loss is calculated by Woschni's relation.

Combustion model. Combustion process of a spark ignition engine is divided into two processes in general; i.e., the ignition process and the stable flame propagation process. The former is constructed by the flame kernel, which is formed by a spark electric discharge, and the unstable flame propagation of the kernel (9). It is, however, treated as spark ignition delay generally.

In this study, the flame kernel with a 2 mm diameter sphere is given at 0.5-0.6 msec after spark ignition. It is assumed to progress to the stable flame propagation process after that.

Stable flame propagation is characterized by the turbulent entrainment model; i.e., it is divided into a process in which the mixture entrains into burned gas and a chemical reaction process (combustion delay).

The entrainment process was proposed by Blizard and Keck (10), and is represented as follows.

$$\frac{d}{dt} Me = \rho u A f S t \tag{21}$$

$$St = u' + S\ell \tag{22}$$

where Af is flame front area, and where St and S_ℓ represent turbulent and laminar flame velocity respectively.

Combustion rate is calculated by using the characteristic reaction time τc for Taylor microscale λ, this calculation has been developed by Tabaczynski et al. (11).

$$\frac{d}{dt} Mb = (Me - Mb)/\tau c \tag{23}$$

$$\tau c = \lambda/S\ell \tag{24}$$

Taylor microscale has a relationship with turbulent Reynolds number.

$$\lambda/L = C\lambda Ret^{-1/2} \tag{25}$$

$$Ret = u'L/\nu t \tag{26}$$

Laminar flame velocity is calculated by the experimental equation of Keck et al. (12).

$$S\ell = S\ell o\ (\phi)\ (Tu/298)^{\alpha(\phi)}\ P^{\beta(\phi)}\ (1-2.1f) \tag{27}$$

where S_ℓ is laminar flame velocity at 298°K and 1 atm, exponents α and β are functions of equivalent ratio ϕ, and parameter f represents a residual gas fraction.

Flame thickness. Many studies of laminar flame thickness have been done, and the following equation is well-known (9), (13).

$$\delta\ell = \delta p + \delta r = \frac{4.6}{S\ell\rho u Cp} + \frac{\mu}{S\ell\rho u\ Cp} \frac{Tb - Tig}{Tig - Tu} \sim \frac{\mu}{Cp} \frac{1}{\rho u S\ell} \tag{28}$$

δp and δr are preheat and reaction zone respectively. μ is a thermal conductivity, and Tig is temperature at ignition.

In this study, furthermore, the following turbulent flame thickness, which is defined as mixture entrainment during the reaction time τc per unit density and flame front area, has been assumed.

$$\delta t = \frac{Me\ (t + \tau c) - Me(t)}{\rho u \cdot Af} \tag{29}$$

Introducing entrainment rate per unit time Me, eq. (29) can be changed to eq. (30).

$$\delta t = \frac{Me}{\rho u \cdot Af}\ \tau c \tag{30}$$

Substituting eq. (24) into eq. (30),

$$\delta t = \frac{Me \cdot \lambda}{Af} \frac{1}{\rho u \cdot S\ell} \tag{31}$$

eq. (30) becomes the same type as eq. (28). When the turbulent intensity becomes zero without limit; i.e., $u' \longrightarrow 0$, we have

$$\delta t \longrightarrow \lambda \tag{32}$$

from eqs. (21) and (22). Eq. (32) indicates that laminar flame thickness is one Taylor microscale size. It is thought to be a reasonable result, then the defined equation (29) is thought to be reasonable.

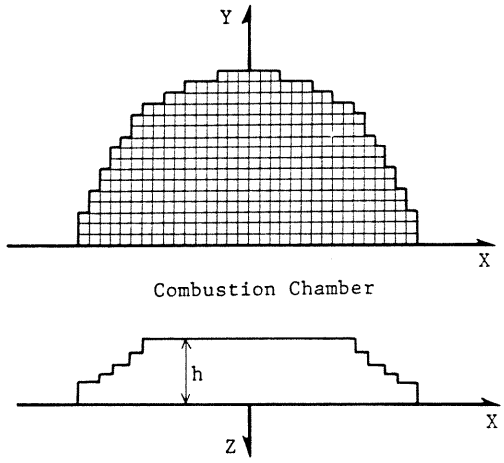

Fig.3 Flame Propagation Model

Flame front area. In the case of a cylindrical combustion chamber, flame front area can be calculated easily from burned gas volume. In the case of a hemi-spherical chamber or more complex chambers and in the case of an investigation of spark plug location, a special way is required to calculate the flame front area.

The following model has been made to obtain the relation between flame front area and burned gas volume. The horizontal plane is divided into a two dimensional mesh and depth of combustion chamber h is given to each mesh as shown in Fig. 3, assuming that a combustion chamber is shallow enough (1), (14).

In this study, a cylindrical combustion chamber is assumed when in-cylinder flow is calculated. This model is only used for an investigation into spark plug location as it is not reasonable to apply it to hemi-spherical or more complex chambers.

MEASUREMENT OF IN-CYLINDER FLOW

The in-cylinder flow of an engine with the specifications summarized in Table 1 has been measured by means of Hot Wire anemometer, and the mean flow velocity and the turbulence intensity have been analized.

Table 1 Engine Specifications

Bore	77 mm
Stroke	80 mm
Swept Volume	372.5(x4) cc
Compression Ratio	9.0
Combustion Chamber	Hemi-spherical

Table 2 Specifications of Hot Wire Probe

Type	Cross Flow Type with 2 Wires
Material	Pt-Ir
Diameter x Length	6.3(μm) x 1.25(mm)

Hot Wire Anemometer

Fig. 4 and Table 2 show a block diagram of a Hot Wire anemometer apparatus and the specifications of a Hot Wire probe used in measurements.

Because a Hot Wire signal requires compensations for gas temperature and pressure, gas temperature and pressure were also measured simultaneously. In order to measure gas temperature, a cross flow type probe with two wires was used. One of the two wires was used for gas flow, and the other was used for gas temperature. The temperature of the flow signal can be compensated for when the temperature signal which runs through a temperature compensator is input into the Hot Wire anemometer, as shown in Fig. 4.

The pressure signal was measured by means of a pressure transducer and a charge amplifier (Kistler type 601A and 5007). In order to compensate for pressure, the flow signal was divided by the pressure signal (16).

A constant temperature type anemometer was used, and the flow signal was linearized according to King's equation (KANOMAX System 7224).

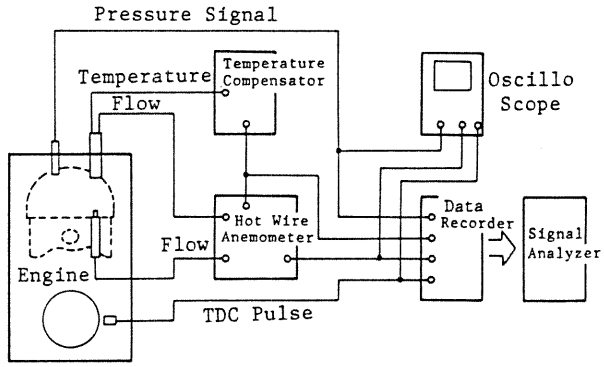

Fig.4 Block Diagram of Hot Wire Anemometer Apparatus

Measuring Method

Fig. 5 shows the measuring points. There are a few points to attach a probe in case of an actual engine. Three measuring points were selected; a spark plug electronode position (P) on the cylinder head side, and two positions (A & B) on the piston crown.

One of the two wires of the probe was fixed to face the swirling flow at a right angle, and swirl velocity was measured.

The flow signal at points A and B were taken out from a cylinder block by means of Link Method. To draw two sealed copper wires out of the engine from a probe attached to a piston, as shown in Fig. 5, was too difficult. We therefore drew out only one wire for the flow signal. The temperature of the flow signal was compensated by the temperature signal of the probe attached at the spark plug position (P).

Engine operating condition is mortoring, 1500 rpm and 45% volumetric efficiency.

Analysis of In-cylinder Flow (17), (18), (19)

The mean flow velocity $\overline{U}$ is calculated by an ensemble mean of a 100 cycles' flow signal; i.e.,

$$\overline{U}(\theta) = \frac{1}{N} \sum_{i=1}^{N} Ui(\theta) \qquad (33)$$

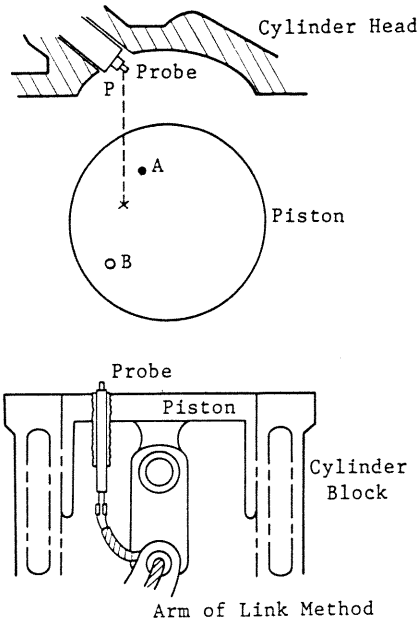

Fig.5 Measuring Points with Hot Wire Probes

where N is selected 100, θ is a crank angle, and Ui (θ) is a one cycle flow signal.

The turbulence intensity is defined as the following ensemble mean value.

$$u' = \sqrt{\frac{1}{N}\sum_{i=1}^{N}[Ui(\theta) - U(\theta)]^2} \qquad (34)$$

When we take out more than 50 - 100 Hz components of flow signals through a high pass filter and take an ensemble mean value, we can obtain the turbulence intensity data which is almost the same value as the one obtained from eq. (34). In this study, in any case, the turbulence intensity was calculated according to eq. (34).

One more important characteristic of turbulence is the integral scale Lt which is generally defined as follows.

$$R(\tau) = \frac{1}{\Delta T}\int_0^{\Delta T} \frac{u'(t)\cdot u'(t+\tau)}{\overline{u'^2}}\, dt \qquad (35)$$

$$Lt = \int_0^{\Delta T} R(\tau)\, d\tau \qquad (36)$$

where τ is correlation time, and where R(τ) is a self-correlation function.
Though the profile of R (τ) becomes more stable as a larger ΔT is set, we set ΔT as 45° C.A. (5 msec at 1500 rpm) and obtained the integral scale because the variation of the integral scale in a cycle is required.

The integral length scale is calculated by the Taylor assumption;

$$L = Lt \cdot \overline{U}_{\Delta T} \qquad (37)$$

$$\overline{U}_{\Delta T} = \frac{1}{\Delta T}\int_0^{\Delta T} \overline{U}(\theta)\, dt \qquad (38)$$

RESULTS AND DISCUSSIONS

In-Cylinder Flow

Because the test engine has a hemi-spherical combustion chamber and the engine in calculation has a cylindrical one, it is not possible to strictly compare between the measurements and the calculations. However, a cavity with a diameter of 72 mm is supposed to be a combustion chamber (squish area is 12.5%) in case of the calculated engine, according to the decrease rate of mean flow velocity during a compression stroke.

Fig. 6 shows the comparison of mean flow velocities. Measurements are of the mean flow velocities at a point P which is on the cylinder head side and a point A on the piston crown side as shown in Fig. 5. Though these measurements and calculations are in agreement for a compression stroke, measurement at P is particulary different from the others for an induction stroke, because a Hot Wire probe also picks up the flow in a vertical direction. This influence appears especially at the beginning of an induction stroke. The mean flow velocity at A agrees well with the calculations in general.

Fig. 7 shows the comparison of turbulence intensities. Measurement at point B, which is on the piston crown, is compared with the calculation, as are measurements of points P and A. The calculation is in agreement with the mean value of the measurements at points A and B during induction and compression strokes. The measurement at P is not so different from the others in case of mean flow velocity because the turbulence field is comparably uniform.

Using the same method as for Fig. 7, comparison of integral length scale is shown in Fig. 8. The integral length scale of measurement and calculation are defined as eq. (33) and (14). Though the measurements on the piston crown are in agreement with calculation, measurement at P differs greatly from others. This is a reasonable result because of eq. (37) and data of the mean flow velocity shown in Fig. 6.

It's can be seen from Fig. 6 to Fig. 8, measurements on the piston crown agree well with the calculations. This means that swirl becomes main flow on the piston crown.

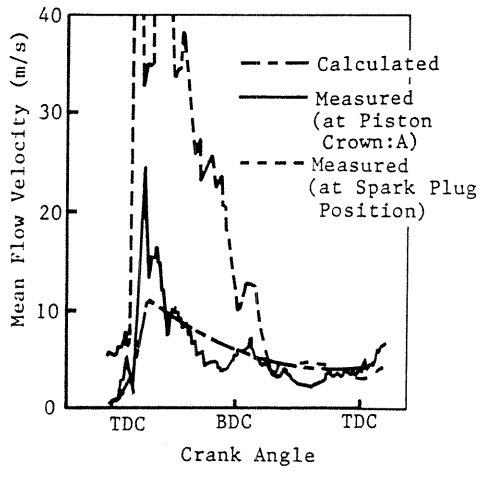

Fig.6 Comparison of Mean Flow Velocity

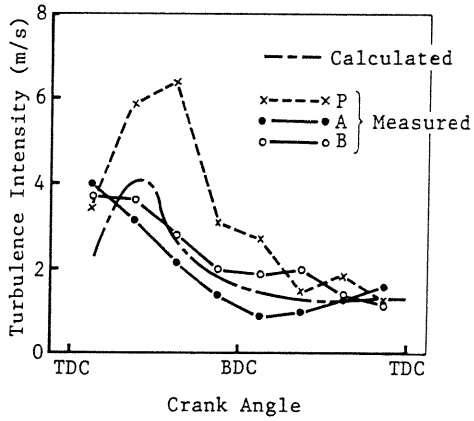

Fig.7 Comparison of Turbulence Intensity

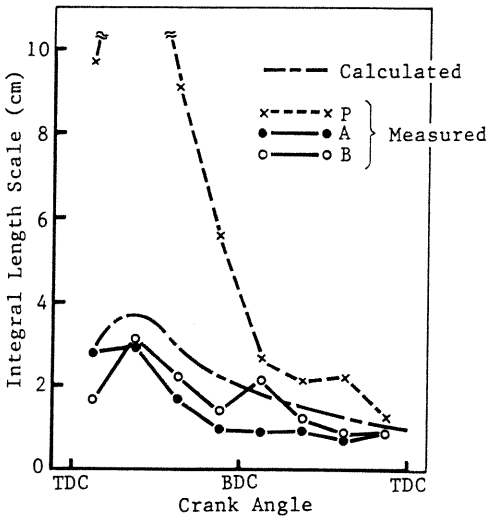

Fig.8 Comparison of Integral Length Scale

Table 3 Base Operating Condition

Engine Speed	1500 rpm
Ignition Timing	20° BTDC
Charging Efficiency	45 %
Air-Fuel Ratio	16.5
Residual Gas Fraction	12 %

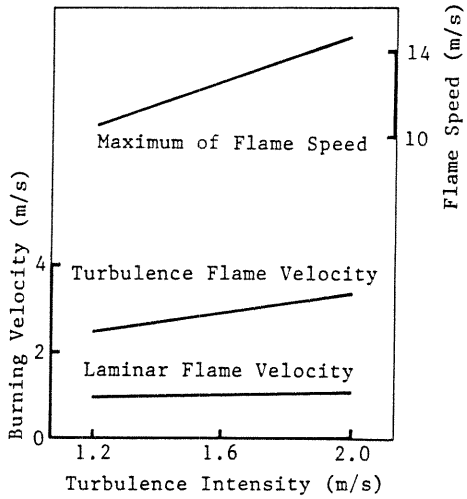

Fig.9 Influence of Turbulence Intensity on Burning Velocity (Base Operating Condition)

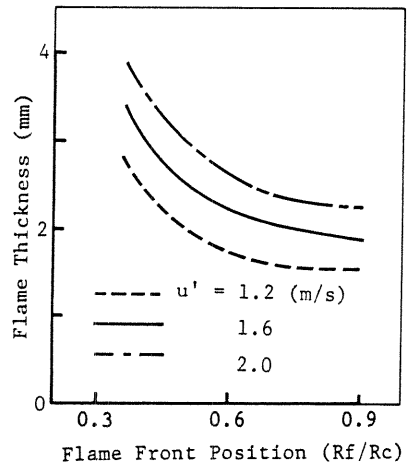

Fig.10a Influence of Turbulence Intensity on Flame Thickness (Base Operating Condition)

Burning Velocity and Flame Thickness

The turbulence intensity and residual gas have strong influences on the turbulent and laminar flame velocity as can be seen from eqs. (21) and (22). The influences of these factors on burning velocity and flame thickness have been investigated by calculation.

Fig. 9 shows the relations between turbulence intensity and burning velocity. The turbulence intensity and the turbulent flame velocity have a good correlation, because the former directly affects the latter. The laminar flame velocity is slightly affected by the turbulence intensity through the influences of gas temperature and pressure which are changed by the increase of turbulent flame velocity. The flame speed is calculated from the variation of burned gas volume, and its maxima are plotted in Fig. 9.

The influences of turbulence intensity and residual gas on flame thickness are shown in Fig. 10a and Fig. 10b. Though the turbulence intensity and residual gas have opposite tendencies for burning velocity, their influences on flame thickness have similar tendency. Because the former increases the mixture entrainment into the flame front, and the latter retards the burning velocity in the flame front, then the flame thickness thickens in both cases.

It is well-known that the ratio of turbulent and laminar flame velocity (S_t/S_ℓ) is an important

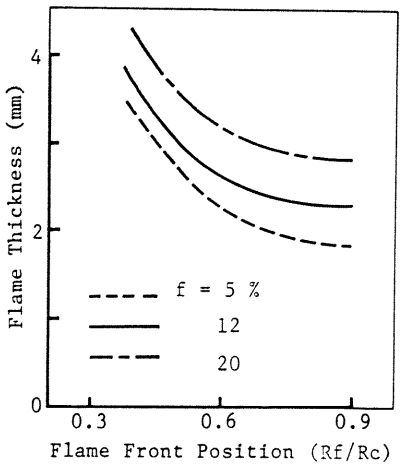

Fig.10b Influence of Residual Gas Fraction on Flame Thickness (Base Operating Condition)

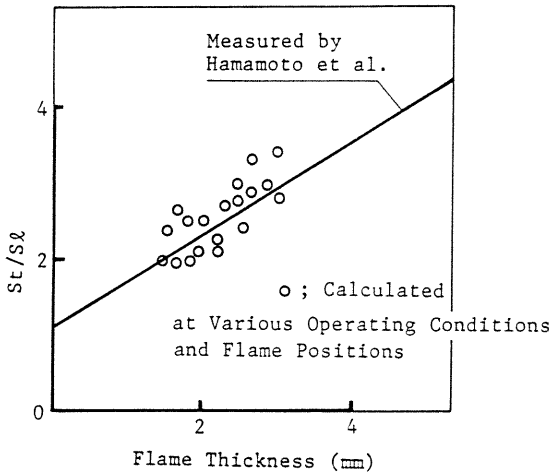

Fig.11 Relation between St/Sℓ and δt

parameter. Hamamoto et al. have studied in detail relations between St/Sℓ and Reynolds number of flame thickness in measurements (13). In this study, the relation between St/Sℓ and flame thickness δt has been investigated in calculations. Fig. 11 shows the comparison between the calculations of this study and the measurements of Hamamoto et al. Calculation conditions are set for a wide range of the turbulence intensity, residual gas fraction and air-fuel ratio in order to change St/Sℓ greatly. Each small circle in Fig. 11 indicates one of these conditions. St/Sℓ is proportional to δt in calculation as well as in measurement. Their absolute values are also in agreement. This result indicates that the entrainment model and the turbulent flame thickness equation introduced in this study are reasonable.

Effect of In-Cylinder Flow and Spark Plug Location

Swirl. Because controlling swirl is comparatively easy and an effective way to hold turbulence energy, it is widely used not only for test engines but also for practical engines. However, it has been reported that the thermal efficiency deteriorates reversely under strong swirl condition, which is an interesting phenomenon (20).

This phenomenon has been studied by calculations in this study. The results are shown in Fig. 12 which represents the indicated mean effective pressure (Pi), burn time and the increasing ratio of heat loss and turbulence intensity. The data of swirl and turbulence intensity are the values at TDC. Heat loss data are the mean values during combustion.

In calculation, the indicated mean effective pressure also slightly deteriorates under high swirl ratio. The reason for this phenomenon is thought to be as follows: the increasing rate of turbulence intensity becomes lower and the improving rate of burn time also becomes lower; on the other hand, when the increasing rate of heat loss becomes larger because of high swirl, then Pi decreases reversely at high swirl region.

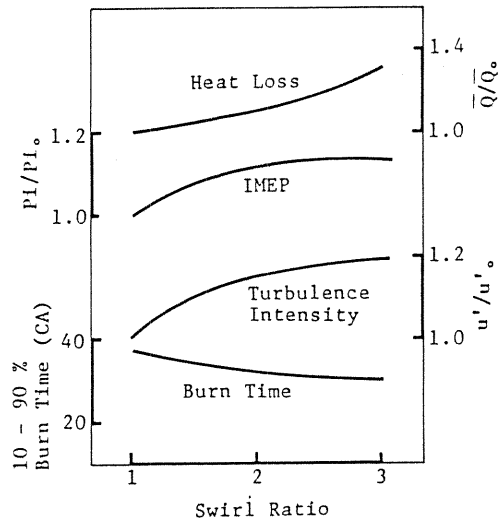

Fig.12 Effect of Swirl (Ignition Timing:MBT, A/F:18)

Squish area. Squish as well as swirl requires attention to gain a method to make turbulence. Especially in a cup-in-piston type combustion chamber, swirl and turbulence are greatly affected by changing the squish area (21).

The effects of the squish area have also been investigated in this study by changing the ratio of the diameter and the depth of cavity under the same compression ratio.

Fig. 13 shows the results. According to the increase of squish area, swirl and turbulence become stronger and burn time shortens. However, there is the maximum of the indicated mean effective pressure. In general, this phenomenon is explained by the increase of heat loss. However, the following explanation may apply:

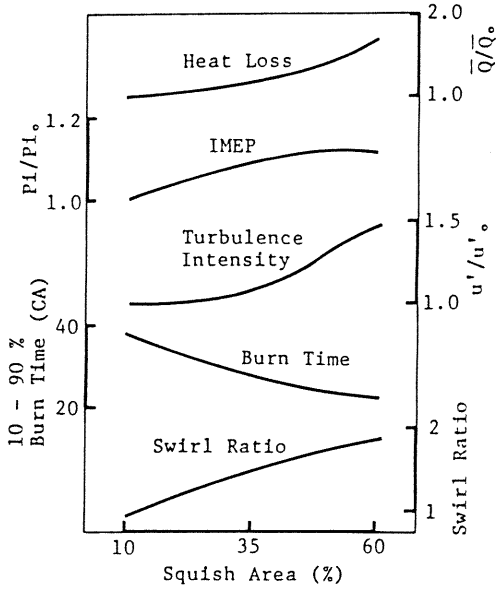

Fig.13 Effect of Squish Area
(Ignition Timing:MBT, A/F:18)

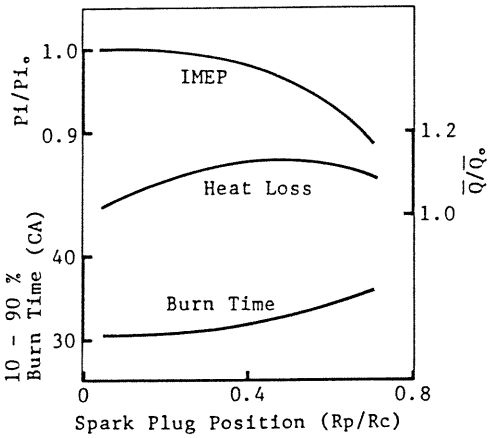

Fig.14 Effect of Spark Plug Location
(Ignition Timing:MBT, A/F:18)

because the flame thickness is thickened by the increase of turbulence as shown in Fig. 10a, the entrainment term in the energy conservation eq. (15), which does not contribute to the work, becomes larger. The thermal efficiency, then, deteriorates.

Spark plug location. The effect of spark plug location, especially that of a centrally located spark plug under low swirl, is well-known. Fig. 14 shows the calculations of the effects. The entrainment of the mixture is promoted by the turbulence flame velocity or the flame front area. The aim of swirl and squish is to increase the speed of the former. On the other hand, the aim of spark plug location is to increase the size of the latter. The increase of flame front area presents the same effects as the increase of burning velocity. Swirl and squish enlarge heat loss from the wall or surface of the combustion chamber directly. This is not taken into account perfectly in this model. When a spark plug is located at the center of the combustion chamber, however, heat loss to the wall decreases, because the flame arrives at the cylinder wall at the end of combustion.

To locate a spark plug near the center of combustion chamber is an effective way to improve thermal efficiency, especially under low swirl.

CONCLUSION

Through the development of this engine simulation model and the measurement of in-cylinder flow, the following conclusions have been reached.

(1) The in-cylinder flow model, which is made by coupling the K-ε model and the wall shear, predicts swirl and turbulence well and is a practical model.

(2) The swirl component becomes the main flow on the piston crown even in the induction stroke.

(3) The turbulent entrainment model and the turbulent flame thickness introduced in this study explain the combustion structure well.

(4) The ratio of turbulent and laminor flame velocity St/Sℓ and the turbulent flame thickness δt have a good correlation.

(5) The phenomenon that the thermal efficiency deteriorates at the high swirl region, is explained by the decrease of the increasing ratio of turbulence intensity and the increase of the heat loss from the wall.

(6) Squish area and spark plug location, which affect not only in-cylinder flow but also geometrical flame propagation, as well as swirl are effective parameters to improve the thermal efficiency. To combine these parameters in the best possible way is desirable.

NOMENCLATURE

A = area
Cp = specific heat at constant pressure
D = destruction of structure
E = internal energy
f = residual gas fraction
H = specific enthalpy
J = diffusion of structure
K = turbulent kinetic energy
L = integral length scale
Lt = integral time scale
M = mass
P = pressure, production of structure
Q = heat loss
R = radius
Rc = bore
Rb = radius of cavity
Ret = turbulent Reynolds number
R(τ) = self-correlation function
Sℓ = laminar flame velocity
St = turbulent flame velocity
T = temperature

Ts = shear stress
u' = turbulence intensity
$\bar{U}$ = mean flow velocity
Uθ = swirl speed
V = volume
W = work
γ = specific heat ratio
δ = flame thickness
ΔT = time interval
ε = dissipation of turbulent kinetic energy
λ = Taylor microscale
μ = thermal conductivity
νt = turbulent kinematic viscosity
ρ = density
τ = correlation time
τc = characteristic reaction time for the microscale
ϕ = equivalence ratio
Ω = specific angular momentum

Subscripts

b = burned gas
c = cylinder
e = entrainment
ex = exhaust
f = flame
i = b or u, in or ex, number
in = induction
ℓ = laminor
P = plug
t = turbulent
u = unburned gas, upstream

REFERENCES

1. Basso, A., Rinolfi, R., "Two-Dimensional Computations of Engine Combustion: Comparison of Measurements and Predictions," SAE Paper No. 820519, 1982.

2. Diwaker, R., "Assessment of the Ability of a Multi-dimensional Computer Code to Model Combustion in a Homogeneous-Charge Engine," SAE Paper No. 840230, 1984.

3. Sherman, R.H., and Blumberg, P.N., "The Influence of Induction and Exhaust Processes on Emissions and Fuel Consumption in the Spark Ignited Engine," SAE Paper No. 770880, 1977.

4. Uzlean, T., Borgnakke, C., and Morel, T., "Characterization of Flow Produced by a High-Swirl Inlet Port," SAE Paper No. 830266, 1983.

5. Borgnakke, C., Davis, G.C., and Tabaczynski, R.J., "Prediction of In-Cylinder Swirl Velocity and Turbulence Intensity for an Open Chamber Cup in Piston Engine," SAE Paper No. 810224, 1981.

6. Davis, G.C., and Borgnakke, C., "The Effect of In-Cylinder Flow Processes on Engine Efficiency - Model Predictions," SAE Paper No. 820045, 1982.

7. Hires, S.D., Tabaczynski, R.J., and Novak, J.M., "The Prediction of Ignition Delay and Combustion Intervals for a Homogeneous Charge, Spark Ignition Engine," SAE Paper No. 780232, 1978.

8. Hiraki, H., and Rife, J.M., "Performance and NOx Model of a Direct Injection Stratified Charge Engine," SAE Paper No. 800050, 1980.

9. Kumagaya, S., Combustion, in Japanese, Iwanami Press, Tokyo, 1976.

10. Blizard, N.C., and Keck, J.C., "Experimental and Theoretical Investigation of Turbulent Burning Model for Internal Combustion Engines," SAE Paper No. 740191, 1974.

11. Tabaczynski, R.J., Ferguson, C.R., and Radhakrishman, K., "A Turbulent Entrainment Model for Spark-Ignition Engine Combustion," SAE Paper No. 770647, 1977.

12. Metghalchi, M and Keck, J.C., "Burning Velocities of Mixtures of Air with Methanol, Isooctane, and Indolene at High Pressure and Temperature," Combustion and Flame 48: PP. 191-210, 1982.

13. Hamamoto Y., Ohkawa, H., Yamamoto, H. and Sugahara, R., "Effects of Turbulence on Combustion of Homogeneous Mixture of Fuel and Air in Closed Vessel," Bulletin of the JSME, vol. 27, No. 226, pp. 756-762, 1984.

14. Poulos, S.G., and Heywood, J.B., "The Effect of Chamber Geometry on Spark-Ignition Engine Combustion," SAE Paper No. 830334, 1983.

15. Lucas, G.C., James, E.H., and Anton, R., "Calibration of a Hot Wire Anemometer for Use in 'Motored' Engines," ASME, the Energy Technology Conference & Exposition, New Orleans, Feb. 3-7, 1980.

16. Aramaki, U., Shibata, S., and Inoue, T., "Unsteady and High Temperature Gas Flow Measurements by Hot Wire Anemometer with Two-Wire Probe 1st report," in Japanese, JSAE, 1982.

17. Murata, S., et al., Foundation and Application of LDV, in Japanese, Nikkan Kohgyo Press, Tokyo, 1980.

18. Lancaster, D.R., "Effect of Engine Variables on Turbulence in a Spark Ignition Engine," SAE Paper No. 760159, 1976.

19. Matuoka, S., Kamimoto, T., Nagakura, K., and Aoyanagi, T., "In-Cylinder Flow Measurements by LDV (Study of Turbulence Measurements and Back-Scattered LDV)," in Japanese, Joint Symposium on Internal Combustion Engines, pp. 55-60, 1979.

20. Nagao, A., and Tanaka, K., "The effect of swirl control on combustion improvement of spark ignition engine," IME paper C54/83, 1983.

21. Kono, S., and Nagao, A., "Prediction of the Combustion Characteristics by Spray and Combustion Model for Direct Injection Diesel Engine," JSAE Review, November pp. 8-14, 1984.